Naunyn-Schmiedeberg's Archives of Pharmacology
https://doi.org/10.1007/s00210-026-05492-6

RESEARCH

Calcium hydroxide nanoparticles-induced oxidative stress and mitochondrial impairment drive genomic instability and programmed cell death in colorectal cancer cells

Hanan R. H. Mohamed[1] · Rawan S. Hekal[2] · Chahd W. H. Fahmy[2] · Shahd O. Elhaggan[2] · Zeina Noure[2] · Nada Ahmed[2] · Ayman Diab[2] · Gehan Safwat[2]

Received: 24 April 2026 / Accepted: 15 May 2026

Abstract

The high aggressiveness, metastatic potential, and mortality of colorectal cancer, together with the limitations of conventional chemotherapy, highlight the urgent need for safer and more effective therapeutic alternatives. Nanotherapies offer promising advantages through improved bioavailability and tumor targeting. In particular, calcium hydroxide nanoparticles ($Ca(OH)_2$NPs) possess unique physicochemical properties, yet their anticancer potential in colorectal cancer remains fully unexplored. This study was consequently undertaken to estimate the cytotoxic effects and underlying molecular mechanisms of $Ca(OH)_2$NPs in human colorectal HCT-116 cancer cells, while also exploring their impact on the viability of normal human HFB4 melanocytes. Normal HFB4 and cancerous HCT-116 cells were exposed to serial two-fold concentrations of $Ca(OH)_2$NPs ranging from 7.80 to 1000 mg/ml for 72 h, and cell viability was assessed using the MTT assay. Intracellular reactive oxygen species (ROS) generation and mitochondrial membrane potential were measured using 2′,7′-dichlorodihydrofluorescein diacetate (DCFH-DA) and rhodamine-123 staining, respectively. Genomic DNA damage was evaluated by the alkaline comet assay, whereas apoptosis induction was analyzed using DAPI staining and the chromatin diffusion assay. The expression levels of mitochondria- and apoptosis-related genes were quantified by quantitative real-time PCR (qRT-PCR). Results of the MTT assay demonstrated that $Ca(OH)_2$NPs exerted significant, dose-dependent cytotoxicity on colorectal HCT-116 cancer cells, as evidenced by a markedly low IC50 value of 35.04 µg/ml and a substantial reduction in cell viability. In contrast, the viability of normal HFB4 melanocytes was only slightly affected, and only at the highest $Ca(OH)_2$NPs concentration tested, as indicated by a comparatively high IC50 value of 190.80 µg/ml. The resulting selectivity index of 5.44 further supports the notable cytotoxicity of $Ca(OH)_2$NPs toward HCT-116 colorectal cancer cells. Furthermore, treatment of HCT-116 cells with $Ca(OH)_2$NPs at the IC50 concentration (35.04 µg/ml) led to a significant increase in intracellular ROS generation level, dramatic loss of mitochondrial membrane potential, and pronounced oxidative DNA damage, ultimately culminating in apoptotic cell death. qRT-PCR analysis also demonstrated significant downregulation of both the apoptotic *p53* and the anti-apoptotic *Bcl-2* gene expression, alongside significant upregulation of the mitochondrial *ND3* gene expression. These molecular alterations support the involvement of mitochondrial dysfunction and apoptosis-related gene modulation in the observed $Ca(OH)_2$NPs-induced cytotoxic effects. Conclusion: $Ca(OH)_2$NPs demonstrate notable anticancer activity against human colorectal HCT-116 cancer cells, primarily through ROS-mediated oxidative stress, genomic DNA damage, mitochondrial dysfunction, and apoptosis induction. These findings highlight $Ca(OH)_2$NPs as a potent nanotherapeutic candidate for colorectal cancer management. However, the current study was limited to in vitro experimental conditions, and the precise molecular mechanisms underlying these effects remain incompletely understood. Therefore, further mechanistic investigations, advanced in vitro and in vivo studies, and comprehensive biocompatibility and safety evaluations are required to validate their therapeutic potential and clinical applicability.

Keywords HCT-116 cancer cells · $Ca(OH)_2$NPs · Cytotoxicity · Oxidative stress · Genomic instability · Mitochondrial dysfunction and apoptosis induction

Extended author information available on the last page of the article

Published online: 04 June 2026

Introduction

Colorectal cancer is one of the most prevalent and life-threatening malignancies worldwide, representing a major cause of cancer-related morbidity and mortality in both developed and developing countries. According to global cancer statistics, colorectal cancer ranks among the top three most commonly diagnosed cancers and remains a leading cause of cancer-associated deaths, with incidence rates steadily rising in many regions due to aging populations and lifestyle factors such as obesity, physical inactivity, smoking, alcohol use, and low-fiber, high–red meat diets (Rawla et al. 2019; Xi and Xu 2021; Lao and Grady 2011). Colorectal cancer arises from the stepwise accumulation of genetic and epigenetic alterations that drive the transformation of normal colonic epithelium into adenomatous polyps and eventually invasive carcinoma. This multistep carcinogenic process involves dysregulation in oncogenes, tumor suppressor genes, and DNA repair genes, resulting in disruption of critical pathways that control cell proliferation, apoptosis, mitochondrial function, and genomic stability. Collectively, these molecular alterations promote tumor initiation, progression, and resistance to therapy (Anbari and Ghanadi 2025; Jung et al. 2020; Gharib and Robichaud 2024).

Despite the availability of multiple treatment strategies for colorectal cancer, including surgical resection, radiotherapy, chemotherapy, targeted therapy, and immunotherapy, chemotherapy remains the primary approach for advanced and metastatic disease, commonly using agents such as 5-fluorouracil, oxaliplatin, and irinotecan. However, conventional chemotherapy is severely limited by systemic toxicity, non-selective action against rapidly dividing cells, severe side effects, the emergence of drug resistance, and reduced efficacy in advanced or recurrent cases (Anand et al. 2022; Fadlallah et al. 2024; Zafar et al. 2025). These significant drawbacks highlight the urgent need for novel therapeutic strategies that are safer, more selective, and capable of specifically targeting cancer cells while sparing normal tissues. In response, current research is increasingly focused on developing innovative approaches, including nanomedicine, targeted molecular therapies, and agents that regulate oxidative stress, apoptosis, and mitochondrial function, with the goal of enhancing efficacy and minimizing treatment-related toxicity (Bishoyi et al. 2025).

Nanotechnology-based therapeutics have emerged as a promising approach in cancer research due to their unique physicochemical properties. Engineered nanoparticles, with their nanoscale size, high surface-to-volume ratio, tunable surface chemistry, and enhanced cellular uptake, allow for improved drug delivery, precise tumor targeting, and modulation of intracellular signaling pathways compared with conventional treatments. Importantly, many nanoparticles have demonstrated intrinsic anticancer activity through the induction of oxidative stress, mitochondrial function disruption, and apoptosis induction (Ammar et al. 2025; Mohamed et al. 2026). Calcium hydroxide nanoparticles ($Ca(OH)_2$NPs) represent a novel and underexplored nanomaterial with distinctive chemical reactivity, biocompatibility, and biological activity. While calcium-based compounds have been widely used in biomedical and dental applications for their antimicrobial and bioactive properties, their potential anticancer effects, especially against colorectal cancer, remain largely unexplored (Rattanakijkamol et al. 2025; Roig et al. 2024).

Recent evidence suggests that $Ca(OH)_2$NPs can selectively target hepatocellular carcinoma Hep-G2 cells and pancreatic PANC-1 cells, leading to elevated intracellular reactive oxygen species (ROS), extensive oxidative DNA damage, disruption of mitochondrial membrane potential, and activation of apoptosis-related signaling pathways, including pro-apoptotic *p53*, mitochondrial *ND3*, and anti-apoptotic *Bcl-2*regulation (Lai et al. 2013; Grzybowska-Szatkowska and Ślaska 2014; Fakeeha et al. 2025). Considering that colorectal cancer cells often exhibit redox imbalance and mitochondrial susceptibility, ROS-mediated strategies using $Ca(OH)_2$NPs may offer a particularly effective and potential therapeutic approach (Mohamed et al. 2025a, b). However, the biological and anticancer potential of $Ca(OH)_2$NPs in colorectal cancer cells remain fully unexplored. There is a notable lack of data regarding their effect on the viability of HCT-116 colorectal cancer cells, their capacity to induce oxidative stress and genotoxic damage, their influence on mitochondrial function, and their ability to modulate apoptosis-related signaling pathways, particularly the *p53*/*ND3*/*Bcl-2* signaling axis, which plays a central role in regulating cell survival and programmed cell death. Moreover, very few studies have investigated the impact of $Ca(OH)_2$NPs on normal human cells, such as HFB4 melanocytes, which is critical for determining their selectivity, cytotoxicity profile, and overall safety as a potential therapeutic agent.

Given the ongoing challenges in colorectal cancer treatment and the increasing interest in nanomedicine, investigating both the anticancer efficacy and safety profile of $Ca(OH)_2$NPs is highly relevant. Accordingly, the present study was designed to systematically assess the biological and anticancer effects of $Ca(OH)_2$NPs in human colorectal HCT-116 cancer cells. The study specifically examines their ability to induce oxidative DNA damage, impair mitochondrial function, trigger pro-apoptotic mechanisms, and modulate critical molecular pathways, including the *p53/ND3/Bcl-2* signaling cascade. Simultaneously, the effects of $Ca(OH)_2$NPs on normal HFB4 melanocyte viability

were assessed to determine their selectivity and safety. By integrating detailed mechanistic studies in cancer cells with cytotoxicity evaluations in normal cells, this research provides novel and detailed insights into the potential of $Ca(OH)_2$NPs as a selective, effective, and innovative nanotherapeutic candidate for colorectal cancer management.

Materials and methods

Chemicals and reagents

The $Ca(OH)_2$NPs white powder was commercially obtained from NanoTech Company (Cairo, Egypt), with a manufacturer-reported average particle size of < 100 nm. Upon receipt, the nanoparticles were stored in tightly sealed containers under dry conditions at room temperature to prevent moisture uptake and physicochemical alteration. Immediately prior to each experiment, the required amount of $Ca(OH)_2$NPs powder was accurately weighed using a calibrated analytical balance to ensure precise dosing. The nanoparticles were then freshly dispersed in dimethyl sulfoxide (DMSO; Sigma-Aldrich, USA) to prepare a concentrated stock solution (1 mg/ml). This stock was subsequently diluted with the appropriate culture medium to obtain the desired working concentrations ranging from 7.80 to 1000 µg/ml. To achieve a homogenous suspension and reduce particle agglomeration, all nanoparticle dispersions were subjected to ultrasonication at 40 kHz for 30 min using a digital ultrasonic bath. This step was carefully standardized across experiments to enhance dispersion stability and ensure reproducible cellular exposure. Vortex mixing was also applied briefly before each use to maintain uniformity of the suspension.

All other chemicals and consumables used throughout the study were of high analytical or molecular biology grade to minimize experimental variability. Key reagents, including DMSO, 3-(4,5-dimethylthiazol-2-yl)−2,5-diphenyl tetrazolium bromide (MTT), and trypan blue dye, were sourced from reputable suppliers and prepared according to the manufacturers' instructions. Reagents were freshly prepared or appropriately stored to maintain stability and performance. Cell culture reagents comprised Dulbecco's Modified Eagle Medium (DMEM), HEPES buffer, L-glutamine, gentamycin, and trypsin–EDTA. The complete growth medium was supplemented with 10% heat-inactivated fetal bovine serum (FBS) and 1% gentamycin to support optimal cell proliferation and prevent bacterial contamination. Phenol red–free medium was employed in experiments involving colorimetric or spectrophotometric measurements to avoid optical interference. All media and solutions were equilibrated to physiological pH and temperature before application to cells. Experimental procedures were carried out under strictly aseptic conditions in a class II biosafety cabinet, following standard sterile cell culture practices. Routine monitoring for contamination and consistent handling protocols were implemented to ensure experimental reproducibility, data reliability, and overall quality control.

Characterization of $Ca(OH)_2$NPs

The physicochemical properties of the $Ca(OH)_2$NPs used in the present study were previously characterized in detail in our recent work (Mohamed et al. 2025a) using complementary analytical techniques. X-ray diffraction analysis confirmed the high crystallinity and phase purity of the nanoparticles, with characteristic diffraction peaks observed at $2\theta \approx 18°$, 29°, and 34°, corresponding to calcium hydroxide and indicating the absence of detectable impurities. Dynamic light scattering analysis showed a zeta potential value of + 2.45 mV, suggesting weak electrostatic repulsion between particles and a tendency toward mild aggregation in aqueous suspension. The polydispersity index was recorded as 0.416, indicating a moderately broad size distribution and partial heterogeneity of the colloidal system. Therefore, ultrasonication was applied prior to biological experiments to ensure adequate dispersion and improve suspension stability.

Morphological characterization using transmission electron microscopy (TEM) further confirmed the nanoscale structure and morphology of $Ca(OH)_2$NPs. The TEM images revealed well-dispersed $Ca(OH)_2$NPs with predominantly cubic to near-spherical shapes, smooth surfaces, and limited aggregation following ultrasonication. Quantitative TEM analysis indicated an average particle size of 12.4 ± 2.4 nm, confirming their nanoscale dimensions with relatively narrow size distribution. Collectively, these previously established characterization results demonstrate that the $Ca(OH)_2$NPs employed in this study possess high crystallinity, defined nanoscale morphology, and moderate colloidal stability. Accordingly, the same well-characterized nanoparticle system reported in (Mohamed et al. 2025a) was used in the present biological investigation.

Culture and propagation of normal HFB4 melanocytes and cancerous HCT-116 colorectal cells

Human colorectal carcinoma HCT-116 cells and normal human melanocyte HFB4 cells were obtained from the Regional Center for Mycology and Biotechnology, Al-Azhar University, Cairo, Egypt. Upon receipt, both cell lines were carefully thawed and gradually adapted to standard sterile culture conditions to ensure optimal recovery, viability, and growth stability. Both HCT-116 and HFB4 cells were cultured in DMEM supplemented with 10% heat-inactivated FBS, providing essential nutrients, growth factors, and

hormones required for cellular proliferation. The medium was further supplemented with antibiotics, including 50 µg/ml gentamycin, 100 U/ml penicillin, and 100 µg/ml streptomycin, to minimize the risk of bacterial contamination. Cells were maintained at 37 °C in a humidified incubator containing 5% CO_2 to ensure physiological pH and optimal growth conditions. The culture medium was replaced every 2–3 days to maintain nutrient availability and eliminate metabolic waste products. Cell morphology, confluence, and overall cellular health were routinely monitored using an inverted phase-contrast microscope. Subculturing was performed when cells reached approximately 70–80% confluence to avoid overgrowth, contact inhibition, and potential phenotypic alterations.

For passaging, cells were washed with phosphate-buffered saline (PBS) and detached using 0.25% trypsin–EDTA. The enzymatic reaction was neutralized with complete culture medium, followed by gentle centrifugation. HFB4 melanocytes and HCT-116 cells were then resuspended and reseeded at appropriate densities according to experimental requirements. Only actively proliferating cells in the logarithmic growth phase were used for all experiments. Cell viability was routinely assessed using the trypan blue exclusion assay, and only cultures with viability $\geq 90\%$ were selected. HCT-116 cells exhibited typical epithelial morphology, while HFB4 melanocytes displayed normal elongated morphology. These standardized conditions were strictly maintained to ensure the accuracy, reproducibility, and reliability of subsequent cytotoxicity, oxidative stress, mitochondrial dysfunction, genotoxicity, and apoptosis assays.

Estimation of $Ca(OH)_2$NPs effect on viability of human normal HFB4 melanocytes and cancerous HCT-116 cells

The cytotoxic potential of $Ca(OH)_2$NPs was examined in human colorectal carcinoma HCT-116 cells and normal human melanocyte HFB4 cells using the MTT assay, a well-established colorimetric method that assesses mitochondrial metabolic activity as an indicator of cell viability. This assay is based on the ability of viable cells to reduce the yellow tetrazolium salt (MTT) into purple, insoluble formazan crystals, reflecting cellular metabolic competence (Mosmann 1983; El-Zahabi et al. 2019; Abdelsalam et al. 2022). Both HCT-116 and HFB4 cells were seeded into sterile 96-well culture plates at a density of 1×10^4 cells per well in 100 µL of complete DMEM enriched with 10% heat-inactivated FBS, 100 U/ml penicillin, 100 µg/ml streptomycin, and 1% L-glutamine to support optimal cell growth. The plates were incubated for 24 h at 37 °C in a humidified atmosphere containing 5% CO_2 to allow proper attachment and stabilization. Following the incubation period, the culture medium was carefully aspirated and replaced with fresh complete DMEM containing graded concentrations of $Ca(OH)_2$NPs (7.8, 15.6, 31.25, 62.5, 125, 250, 500, and 1000 µg/ml). Each concentration was tested in triplicate wells to ensure experimental reproducibility, while untreated control wells received nanoparticle-free medium under identical conditions. The cells were then incubated with $Ca(OH)_2$NPs for 72 h to evaluate dose-dependent cytotoxic effects.

At the end of the exposure period, the medium was removed and replaced with 100 µL of phenol red–free DMEM to avoid interference with absorbance measurements. Subsequently, 10 µL of MTT solution (5 mg/ml in phosphate-buffered saline, PBS) was added to each well, and the plates were incubated for 4 h at 37 °C in the dark. During this period, metabolically active cells reduced MTT to insoluble formazan crystals. After incubation, approximately 85 µL of the supernatant was gently removed, and 50 µL of dimethyl sulfoxide (DMSO) was added to each well to dissolve the formed crystals. The plates were then incubated for an additional 10 min at 37 °C with gentle shaking to ensure complete solubilization. Absorbance was measured at 590 nm using a microplate reader. Cell viability was expressed as a percentage relative to untreated control cells and calculated using the following formula: Cell viability (%) = (ODt/ODc) × 100; where ODt represents the mean optical density of treated wells and ODc represents that of control wells.

The half-maximal inhibitory concentration (IC_{50}) values were calculated using nonlinear regression analysis of the full normalized dose–response data using GraphPad Prism software (variable slope, sigmoidal fit). IC_{50} values were derived from the best-fit curve generated by considering all experimental concentrations rather than visual estimation from plotted graphs. To assess the selectivity of $Ca(OH)_2$NPs toward cancer cells, the selectivity index (SI) was calculated using the equation: SI = IC_{50} (HFB4)/IC_{50} (HCT-116). An SI value greater than 1 indicates potential cytotoxicity toward cancer cells, whereas values less than 1 indicates higher toxicity toward normal cells. All experiments were performed in triplicate and independently repeated at least three times to ensure reproducibility. Data are presented as mean ± standard deviation (SD).

Treatment regimen of HCT-116 cells with $Ca(OH)_2$NPs for molecular analysis

For mechanistic and molecular analysis, human colorectal carcinoma HCT-116 cells were cultured in T25 tissue culture flasks containing DMEM supplemented with 10% heat-inactivated FBS, 1% L-glutamine, and a standard antibiotic mixture (100 U/ml penicillin and 100 µg/ml streptomycin). Cultures were maintained at 37 °C in a humidified incubator with 5% CO_2; and cell growth, morphology, and overall health status were regularly monitored to ensure normal

morphology and consistent proliferation. Cells were allowed to grow until they reached approximately 70–80% confluence, representing the optimal phase for experimental treatment. At this stage, cultures were divided into untreated control cells and $Ca(OH)_2$NPs-treated cells. Control cells were maintained in complete DMEM containing < 0.1% DMSO to exclude any solvent-related effects. In contrast, treated cells were exposed to $Ca(OH)_2$NPs at the predetermined IC_{50} concentration obtained from the MTT cytotoxicity assay.

Both control and treated HCT-116 cancer cells were incubated for 72 h under identical conditions to allow sufficient nanoparticle–cell interaction, cellular uptake, and induction of biological responses. Following the treatment period, cells were detached using 0.25% trypsin–EDTA, collected by centrifugation at 1500 rpm for 5 min at 4 °C, and washed twice with ice-cold PBS (pH 7.4) to remove residual media and unbound nanoparticles. The resulting cell pellets were resuspended in PBS and stored at − 80 °C until further analysis. The collected samples were subsequently used for downstream biochemical and molecular investigations, including estimation of ROS generation level, mitochondrial depolarization, DNA damage, and apoptosis induction. All experiments were conducted in triplicate to ensure reproducibility and statistical reliability of the results.

Estimation of $Ca(OH)_2$NPs effect on genomic DNA stability in HCT-116 cancer cells

The genotoxic potential of $Ca(OH)_2$NPs in human colorectal carcinoma HCT-116 cells was assessed using the alkaline single-cell gel electrophoresis (comet) assay, a highly sensitive and widely validated method for detecting DNA strand breaks and alkali-labile sites (Tice et al. 2000; Langie et al. 2015). This assay enables quantification of DNA damage at the individual cell level, providing a reliable measure of genomic instability following nanoparticle exposure. The suspension of untreated and $Ca(OH)_2$NPs-treated cells was gently mixed with 60 µL of 0.5% low-melting-point agarose maintained at 37 °C. The mixture was immediately layered onto clean microscope slides pre-coated with a thin base layer of 1% normal-melting-point agarose. Slides were allowed to solidify at room temperature for 30 min. The agarose-embedded cells were then lysed by immersion in freshly prepared chilled lysis solution composed of 2.5 M NaCl, 100 mM EDTA, and 10 mM Tris–HCl (pH 10), freshly supplemented with 1% Triton X-100 and 10% DMSO. Slides were incubated at 4 °C in the dark for 24 h to effectively remove cell membranes, nuclear proteins, and other cellular components while preserving the structural integrity of nuclear DNA for subsequent analysis.

Following lysis, slides were equilibrated in alkaline electrophoresis buffer (300 mM NaOH and 1 mM EDTA, pH 12) for 15 min to allow DNA unwinding and conversion of alkali-labile sites into detectable single-strand breaks. Electrophoresis was conducted at 25 V and 300 mA for 30 min at 4 °C to promote migration of fragmented DNA. After electrophoresis, slides were neutralized in 0.4 M Tris–HCl buffer (pH 7.5) for 5 min, dehydrated in chilled ethanol for an additional 5 min, and air-dried. DNA was then stained with 50 µL of ethidium bromide (20 µg/ml) and visualized under a fluorescence microscope. For each experimental group, 50 randomly selected nuclei per slide were analyzed using COMETSCORE™ image-analysis software. DNA damage was quantified using standard comet assay parameters, including tail length, percentage of DNA in the tail, and tail moment, providing a comprehensive assessment of genomic instability. All measurements were performed in triplicate independent experiments, and results were reported as mean ± SD. Statistical analyses were applied to determine the significance of $Ca(OH)_2$NPs-induced genotoxic effects in HCT-116 cells.

Fluorometric analysis of $Ca(OH)_2$NPs-induced oxidative stress in HCT-116 cells

Oxidative stress induction by $Ca(OH)_2$NPs in human colorectal carcinoma HCT-116 cells was assessed through the generation of intracellular reactive oxygen species (ROS). ROS production levels were quantified using the fluorogenic probe 2′,7′-dichlorofluorescin diacetate (DCFH-DA) according to established and widely accepted protocol of Siddiqui et al. (Siddiqui et al. 2010). Following $Ca(OH)_2$NPs exposure, qual volumes of cell suspension and DCFH-DA working solution (final concentration 20 µM) were mixed in sterile microcentrifuge tubes. The mixtures were incubated for 30 min at room temperature in the dark to prevent photobleaching. During this period, DCFH-DA entered the cells and was hydrolyzed by intracellular esterases to form non-fluorescent dichlorofluorescin (DCFH), which is subsequently oxidized by ROS into highly fluorescent dichlorofluorescein (DCF). The resulting fluorescence intensity serves as a quantitative measure of intracellular oxidative stress.

After staining, cells were gently smeared as thin, uniform layers onto pre-cleaned, labeled glass slides. Fluorescence signals were observed using an epifluorescence microscope equipped with appropriate DCF-specific excitation and emission filters. Images were captured at 200 × magnification from randomly selected fields, maintaining consistent exposure and acquisition settings across all samples to allow reliable comparison between treated and control groups. Quantitative analysis of ROS-induced fluorescence was performed using Fiji (ImageJ) software. Mean fluorescence intensity values were calculated for each sample and expressed relative to untreated control cells to assess the extent of $Ca(OH)_2$NPs-induced oxidative stress. All experiments were conducted in triplicate to ensure reproducibility,

and statistical analyses were applied to confirm the significance of ROS generation following nanoparticle exposure.

Estimation of $Ca(OH)_2$NPs on mitochondrial membrane integrity in HCT-116 cells

The influence of $Ca(OH)_2$NPs on mitochondrial membrane potential, a key indicator of mitochondrial functional integrity and an early marker of apoptosis, was evaluated in human colorectal carcinoma HCT-116 cells. Following cell exposure to IC_{50} concentration of $Ca(OH)_2$NPs for 72 h, mitochondrial membrane polarization was assessed using rhodamine-123, a cationic, lipophilic fluorescent dye that selectively accumulates in structurally intact, energized mitochondria (Zhang et al. 2011). Briefly, equal volumes of cell suspension and rhodamine-123 working solution (final concentration 10 µg/ml) were gently mixed in sterile, light-protected microcentrifuge tubes and incubated at 37 °C for 1 h in the dark to allow dye uptake. After staining, cells were washed twice with ice-cold PBS to remove unbound dye and reduce background fluorescence. The stained cells were then carefully mounted onto pre-cleaned glass slides, spread into a thin monolayer, and covered with sterile coverslips.

Fluorescence images were captured using an epifluorescence microscope with appropriate excitation and emission filters for rhodamine-123 at 200 × magnification. Identical imaging parameters were maintained for both $Ca(OH)_2$NPs-treated and untreated control cells to ensure comparability. Quantitative analysis of mitochondrial membrane potential was performed using Fiji (ImageJ) software by measuring mean fluorescence intensity. A decrease in rhodamine-123 fluorescence in treated cells compared to controls was interpreted as mitochondrial depolarization, reflecting mitochondrial dysfunction and early apoptotic events. All experiments were conducted in triplicate, and results were reported as mean ± SD, ensuring reliability, reproducibility, and statistical accuracy.

Detection of $Ca(OH)_2$NPs-induced apoptotic effect in HCT-116 cells

Apoptosis is a tightly regulated form of programmed cell death essential for eliminating damaged or malignant cells and serves as a key indicator of anticancer activity. In this study, the pro-apoptotic effects of $Ca(OH)_2$NPs were investigated in human colorectal carcinoma HCT-116 cells. HCT-116 cells were exposed to $Ca(OH)_2$NPs at the IC_{50} concentration determined by MTT assay and incubated for 72 h to ensure adequate nanoparticle–cell interaction. Untreated cells maintained under identical conditions served as negative controls. Apoptotic induction was evaluated using two complementary approaches, and these experiments were independently conducted in triplicate to ensure reproducibility, reliability, and statistical rigor:

Chromatin diffusion assay: This assay detects late-stage apoptosis by visualizing the characteristic outward migration of fragmented DNA, forming a "halo" around the nuclear core. Microscope slides were first coated with 0.7% normal-melting-point agarose. HCT-116 cell suspensions were mixed with 0.5% low-melting-point agarose (37 °C) and layered onto the pre-coated slides to ensure even distribution. After air-drying, cells were subjected to cold lysis to remove membranes and cytoplasmic components while preserving nuclear structure. Slides were then neutralized with Tris buffer, fixed in chilled ethanol, and stained with ethidium bromide (Singh 2000). Under fluorescence microscopy, apoptotic nuclei were identified by distinct DNA halos, whereas non-apoptotic nuclei remained compact. For each group, 1000 nuclei were analyzed, and the percentage of apoptotic cells was calculated and reported as mean ± SD.

DAPI nuclear staining: To confirm apoptosis and visualize nuclear changes, HCT-116 cells were seeded in 96-well plates (1×10^4 cells/well) and allowed to adhere overnight. After 72-h treatment with $Ca(OH)_2$NPs at IC_{50}, cells were washed with PBS, fixed in 4% paraformaldehyde for 15 min, and incubated with DAPI solution (1 µg/ml in PBS) for 1 h in the dark (Guan 2020). Fluorescence imaging was performed at 200 × magnification using an epifluorescence microscope equipped with appropriate filters. Apoptotic nuclei were distinguished by bright, condensed, or fragmented chromatin, while healthy nuclei exhibited uniform, faint fluorescence with intact morphology. A total of 1000 nuclei per treatment group were scored, and data were expressed as mean ± SD.

Molecular analysis of *p53*, *ND3*, and *Bcl-2* gene expression in $Ca(OH)_2$NPs-treated HCT−116 cells

To gain deeper insight into the molecular pathways underlying the cytotoxic effects of $Ca(OH)_2$NPs, particularly those associated with apoptosis and mitochondrial impairment, quantitative real-time PCR (qRT-PCR) was conducted to quantify the transcriptional expression of selected apoptosis- and mitochondria-related genes. These included the pro-apoptotic tumor suppressor *p53* gene, the mitochondrial ND3 gene (a vital subunit of complex I within the electron transport chain), and the anti-apoptotic *Bcl-2* gene. Human colorectal carcinoma HCT-116 cells were seeded at a density of 1×10^4 cells/well and divided into untreated control and control and $Ca(OH)_2$NPs-treated groups. Treated cells were exposed to the IC_{50} concentration of $Ca(OH)_2$NPs for 72 h. Following treatment, cells were harvested, and total RNA was extracted using the GeneJET RNA Purification

Kit (Thermo Fisher Scientific, USA) in accordance with the manufacturer's instructions. RNA quantity and purity were assessed using a NanoDrop spectrophotometer, and samples with acceptable A260/A280 ratios (1.8–2.0) were used for subsequent analyses.

For cDNA synthesis, 1 µg of total RNA from each sample was reverse-transcribed using the High-Capacity cDNA Reverse Transcription Kit (Applied Biosystems, USA) under standard conditions. Quantitative PCR amplification was subsequently carried out using SYBR Green PCR Master Mix and gene-specific primers listed in Table 1 (Suzuki et al. 1999; Lai et al. 2013; Grzybowska-Szatkowska and Ślaska 2014) on a StepOnePlus Real-Time PCR System (Applied Biosystems, USA). The housekeeping gene*GAPDH* was used as an internal control to normalize gene expression levels. Relative gene expression was calculated using the comparative Ct ($2^{-\Delta\Delta Ct}$) method, enabling comparison between treated and control groups. All reactions were performed in triplicate to ensure accuracy and reproducibility. The obtained data were expressed as mean ± SD, providing insight into the modulation of apoptotic signaling, mitochondrial function, and cell death pathways in response to $Ca(OH)_2$NP exposure in HCT-116 cells.

Statistical analysis

All collected data were statistically analyzed using the Statistical Package for the Social Sciences (SPSS) software. Outcomes derived from the various experimental assays, including DNA damage assessment using the alkaline comet assay, relative gene expression analysis by qRT-PCR, evaluation of mitochondrial membrane potential, measurement of ROS, and apoptosis detection, were expressed as mean ± SD. Differences between $Ca(OH)_2$NPs-treated HCT-116 colorectal cancer cells and their corresponding untreated control cells were evaluated using an unpaired, two-tailed Student's *t*-test. Statistical significance was assigned at a threshold of $p < 0.05$. All experiments were independently performed in triplicate to ensure robustness, reproducibility, and reliability of the obtained results.

Table 1 Sequences of primers used in qRT-PCR

Gene	Strand	Primer's sequences
GAPDH	Forward	5′-GAAGGTGAAGGTCGGAGTCA-3′
	Reverse	5′-GAAGATGGTGATGGGATTTC-3′
ND3	Forward	5′-CGCCGCCTGATACTGGCAT-3′
	Reverse	5′-CTAGTATTCCTAGAAGTGAG-3′
BCL-2	Forward	5′-TCCGATCAGGAAGGCTAGAGT-3′
	Reverse	5′-TCGGTCTCCTAAAAGCAGGC-3′
P53	Forward	5′-CAGCCAAGTCTGTGACTTGCACGTAC-3′
	Reverse	5′-CTATGTCGAAAAGTGTTTCTGTCATC-3′

Results

$Ca(OH)_2$NPs selectively and potently target human HCT-116 colorectal cancer cells

Results of the MTT assay demonstrated that $Ca(OH)_2$NPs exert a strong and targeted cytotoxic effect on HCT-116 colorectal cancer cells. Exposure of HCT-116 cells to a series of two-fold increasing concentrations of $Ca(OH)_2$NPs (7.8, 15.6, 31.25, 62.5, 125, 250, 500, and 1000 µg/ml) for 72 h led to a pronounced, concentration-dependent decline in cell viability as seen in Fig. 1. This progressive reduction reflects a potent inhibitory effect of the nanoparticles on cancer cell proliferation and survival. Quantitative analysis using GraphPad Prism demonstrated a markedly low IC_{50} value of 35.04 µg/ml, indicating high sensitivity of HCT-116 cells to $Ca(OH)_2$NPs treatment and confirming their strong antiproliferative activity.

In contrast, normal HFB4 melanocytes exhibited minimal changes in viability under the same experimental conditions, with only slight cytotoxicity observed at the highest

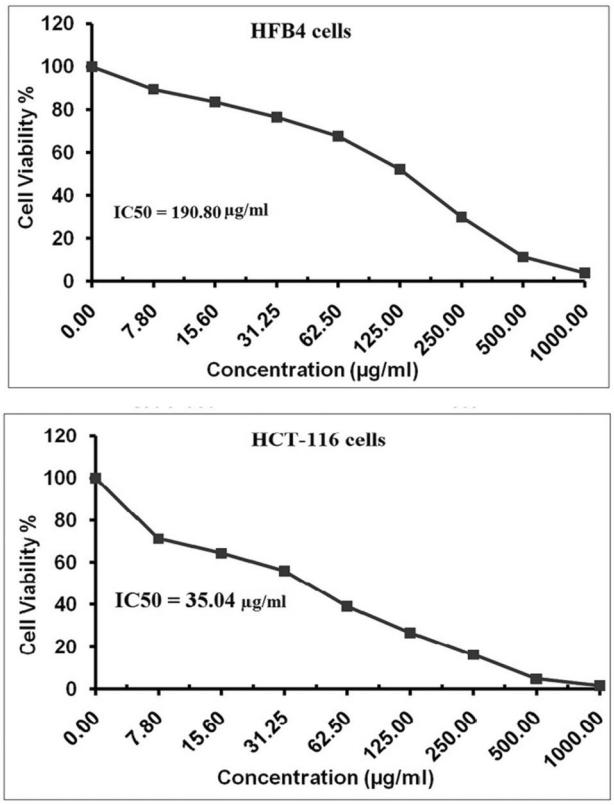

Fig. 1 Viability of human normal HFB4 melanocytes and cancerous HCT-116 colorectal cells measured using the MTT assay following 72-h exposure to $Ca(OH)_2$NPs at serial two-fold increasing concentrations (7.8, 15.6, 31.25, 62.5, 125, 250, 500, and 1000 µg/ml)

$Ca(OH)_2$NPs concentration (1000 µg/ml). Notably, the IC_{50} value in HFB4 cells was considerably higher (190.80 µg/ml), reflecting greater resistance of normal HFB4 cells to $Ca(OH)_2$NPs-induced toxicity. The marked difference in IC_{50} values between cancerous HCT-116 and normal HFB4 cells resulted in a high selectivity index of SI = 5.44, further supporting the potent targeting capability of $Ca(OH)_2$NPs toward malignant HCT-116 cells. Based on this pronounced cytotoxic response, subsequent investigations were directed toward elucidating the underlying molecular mechanisms of action. These included the evaluation of oxidative stress generation, mitochondrial dysfunction, DNA damage, and apoptosis induction.

$Ca(OH)_2$NPs induce severe genomic DNA instability in human HCT-116 colorectal cancer cells

Analysis of the alkaline comet assay results clearly indicated that exposure of human HCT-116 colorectal cancer cells to $Ca(OH)_2$NPs for 72 h at the determined IC_{50} concentration (35.04 µg/ml) resulted in marked genotoxic damage. In comparison with untreated control cells, $Ca(OH)_2$NPs-treated HCT-116 cells exhibited a highly significant increase ($p < 0.001$) in main comet assay parameters, including tail length, percentage of DNA in the tail, and tail moment as depicted in Table 2. These indices collectively reflect extensive DNA strand breaks, alkali-labile sites, and chromosomal fragmentation, confirming a substantial loss of genomic integrity following $Ca(OH)_2$NPs treatment. Treated HCT-116 cells with $Ca(OH)_2$NPs displayed pronounced comet tail elongation and a clear shift of DNA content from the nuclear head toward the tail region, indicating enhanced DNA migration during electrophoresis and, consequently, severe DNA damage. In contrast, untreated control cells retained compact, well-defined nuclei with minimal DNA migration, consistent with preserved genomic stability.

Fluorescence microscopy observations are shown in Fig. 2. Untreated control HCT-116 cells exhibited intact, rounded nuclei with negligible comet formation, indicating preserved genomic stability. In contrast, $Ca(OH)_2$NPs-treated cells displayed classic comet morphologies, featuring well-defined nuclear heads and elongated, diffuse tails. The pronounced tail elongation and evident migration of DNA from the nuclear core into the tail region reflect extensive DNA fragmentation and severe genomic damage, confirming the strong genotoxic effect of $Ca(OH)_2$NPs. The strong concordance between the comet assay measurements and microscopic visualization confirms that $Ca(OH)_2$NPs induce

Table 2 Incidence of genomic DNA damage in human HCT-116 colorectal cancer cells assessed using alkaline comet assay following exposure to the IC_{50} concentration (35.04 µg/ml) of $Ca(OH)_2$NPs for 72 h

Cells	Treatment (concentration)	Tail length (px)	%DNA in tail	Tail moment
HCT-116 colorectal cancer cells	Untreated (0.00 µg/ml)	2.51 ± 0.08	21.18 ± 1.48	0.57 ± 0.06
	$Ca(OH)_2$NPs-treated (35.04 µg/ml)	24.26 ± 2.33***	52.31 ± 3.99***	12.56 ± 0.86***

Triplicates were used and results are expressed as mean ± SD

***Indicates statistical significant difference from the compared untreated control cells at $p < 0.001$, using independent Student t-test

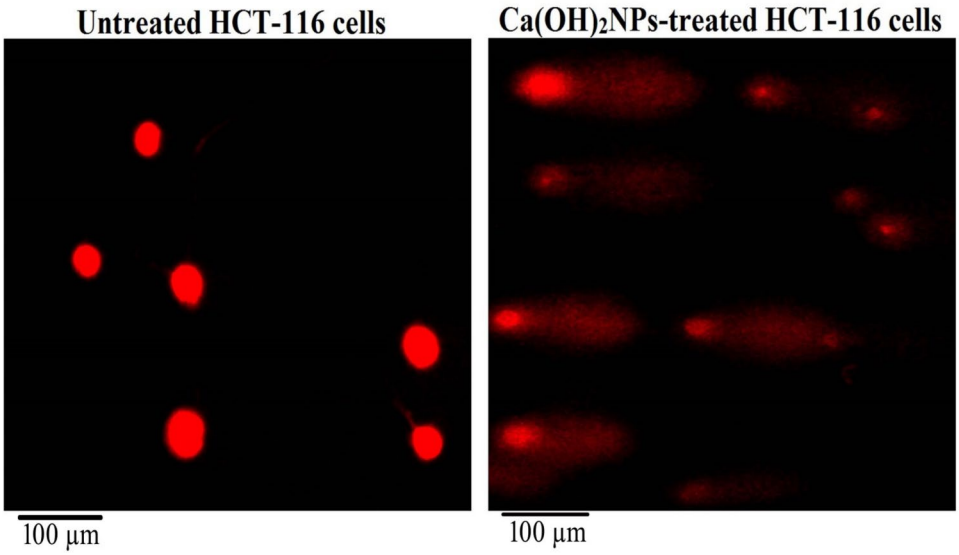

Fig. 2 Examples for the scored comet nuclei with intact DNA in untreated human HCT-116 colorectal cancer cells and those with damaged DNA in HCT-116 cancer cells treated with the IC_{50} concentration of $Ca(OH)_2$NPs (35.04 µg/ml) for 72 h. Magnification 200×

pronounced genomic instability in HCT-116 colorectal cancer cells. Collectively, these results demonstrate that $Ca(OH)_2$NPs exert potent genotoxic effects, leading to extensive DNA damage and chromosomal instability, which likely contribute to their pronounced anticancer activity against colorectal cancer cells.

$Ca(OH)_2$NPs cause marked intracellular oxidative stress in human HCT-116 colorectal cancer cells

Measurement of total intracellular ROS levels using the redox-sensitive fluorescent probe 2′,7′-DCFH-DA demonstrated a robust oxidative response in human HCT-116 colorectal cancer cells following exposure to $Ca(OH)_2$NPs. After 72 h of treatment at the determined IC_{50} concentration (35.04 µg/ml), $Ca(OH)_2$NPs-treated HCT-116 cells exhibited a marked increase in green fluorescence intensity compared with untreated control cells (Fig. 3), indicating substantial intracellular ROS accumulation. Quantitative fluorescence analysis confirmed a highly significant elevation ($p < 0.001$) in ROS levels in treated HCT-116 cells relative to control cells. This increase reflects the oxidation of non-fluorescent DCFH into highly fluorescent DCF in response to excessive ROS generation, confirming the induction of pronounced oxidative stress. In contrast, untreated control cells displayed only weak basal fluorescence, consistent with tightly regulated physiological ROS levels.

Fluorescence microscopy further corroborated these findings. Cancerous HCT-116 cells exposed to $Ca(OH)_2$NPs displayed intense and extensive cytoplasmic fluorescence, indicating markedly increased intracellular ROS production across the $Ca(OH)_2$NPs-treated cell population. In contrast, untreated control cells exhibited weak and homogeneous fluorescence, consistent with the maintenance of normal redox homeostasis (Fig. 3). The pronounced elevation in ROS suggests that $Ca(OH)_2$NPs exposure disturbs intracellular redox

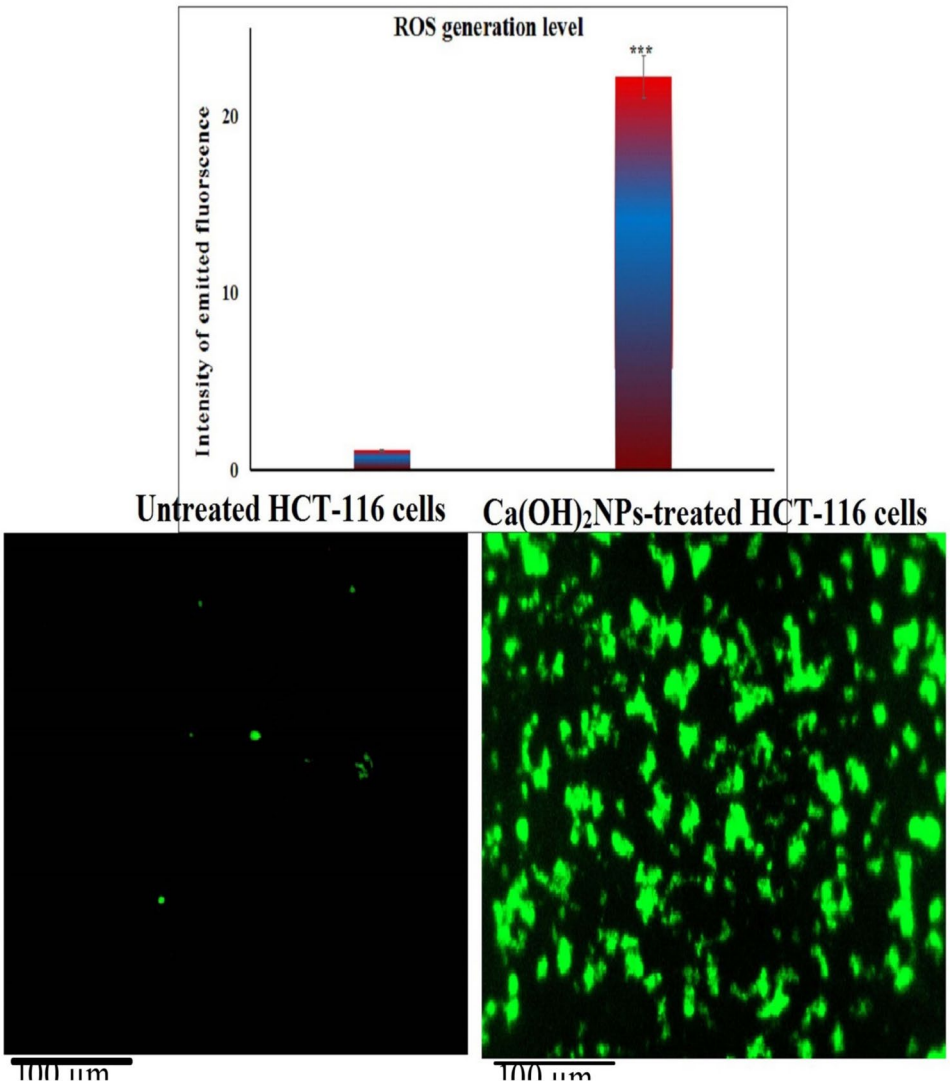

Fig. 3 Qualitative and quantitative assessment of intracellular ROS generation in untreated and $Ca(OH)_2$NPs-treated human HCT-116 colorectal cancer cells using the 2′,7′-DCFH-DA fluorescent probe following 72-h exposure to the IC_{50} concentration (35.04 µg/ml). Fluorescence intensity was quantified using ImageJ software from at least five randomly selected microscopic fields per experimental group, with each experiment performed in triplicate. Images were captured at 200 × magnification

equilibrium and overwhelms the cellular antioxidant defense system. Collectively, these results indicate that $Ca(OH)_2$NPs serve as potent triggers of oxidative stress in colorectal cancer cells. The excessive ROS production likely acts as a critical upstream event leading to oxidative DNA damage, mitochondrial dysfunction, and the activation of apoptotic signaling pathways, thereby contributing significantly to the anticancer effects of $Ca(OH)_2$NPs.

$Ca(OH)_2$NPs cause a dramatic loss of mitochondrial membrane potential in human HCT-116 colorectal cancer cells

Mitochondrial membrane potential was assessed using the cationic fluorescent probe rhodamine-123, which selectively accumulates in active mitochondria with intact electrochemical gradients. Following 72-h exposure of HCT-116 cells to the IC_{50} concentration (35.04 µg/ml) of $Ca(OH)_2$NPs, a marked disruption of mitochondrial function was observed (Fig. 4). A significant decline in rhodamine-123 fluorescence intensity was detected in $Ca(OH)_2$NPs-treated HCT-116 cancer cells compared to untreated control cells, indicating mitochondrial membrane depolarization. Quantitative fluorescence analysis confirmed a highly significant reduction ($p < 0.001$) in dye accumulation in $Ca(OH)_2$NPs-treated cells, reflecting severe impairment of mitochondrial integrity. In contrast, control HCT-116 cells exhibited strong, uniform mitochondrial fluorescence, consistent with preserved membrane potential and normal mitochondrial activity (Fig. 4).

Fluorescence microscopy further supported these findings, as $Ca(OH)_2$NPs-treated HCT-116 cells displayed weak, diffuse, and fragmented fluorescence patterns rather than the distinct, spotted mitochondrial staining observed in untreated control cells (Fig. 4). This alteration suggests substantial disruption of mitochondrial structure and function and is indicative of early activation of intrinsic apoptotic signaling pathways. Collectively, these results demonstrate that $Ca(OH)_2$NPs trigger significant mitochondrial membrane depolarization and dysfunction in HCT-116

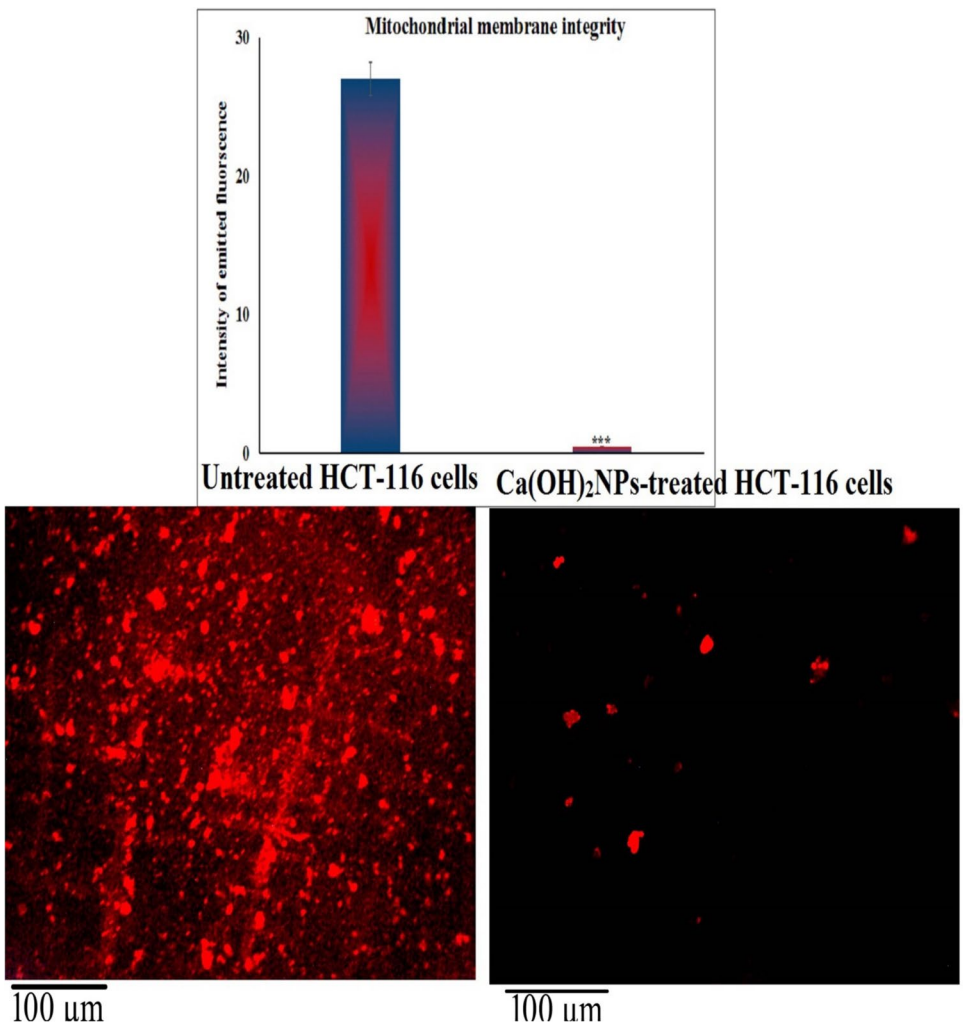

Fig. 4 Qualitative and quantitative analysis of mitochondrial membrane potential in untreated and $Ca(OH)_2$NPs-treated human HCT-116 colorectal cancer cells using rhodamine-123 staining following 72-h exposure to the IC_{50} concentration (35.04 µg/ml). Fluorescence intensity was quantified using ImageJ software from at least five randomly selected microscopic fields per experimental group, with three independent experimental repeats. Images were acquired at 200 × magnification

colorectal cancer cells. The collapse of mitochondrial membrane potential likely represents a key upstream event linking oxidative stress and DNA damage to the initiation of mitochondria-mediated apoptosis, thereby contributing to the strong cytotoxic and anticancer effects of $Ca(OH)_2$NPs.

$Ca(OH)_2$NPs markedly induce apoptosis in human HCT-116 colorectal cancer cells

Findings from both the chromatin diffusion assay and DAPI nuclear staining revealed a significant induction of apoptosis in human HCT-116 colorectal cancer following 72 h of exposure to $Ca(OH)_2$NPs at the IC_{50} concentration (35.04 µg/ml). Under these conditions, $Ca(OH)_2$NPs triggered pronounced nuclear alterations and extensive chromatin degradation, indicative of late-stage apoptotic progression. In the chromatin diffusion assay, apoptotic HCT-116 cells were readily identified by the appearance of prominent chromatin halos surrounding the nuclei. These halos result from the outward diffusion of fragmented DNA into the surrounding matrix under alkaline conditions and represent a well-recognized indicator of apoptosis-associated DNA cleavage. Cells treated with $Ca(OH)_2$NPs showed a marked increase in halo-positive nuclei compared with untreated control cells, which maintained compact and intact nuclei with no detectable chromatin dispersion as depicted in Fig. 5. Quantitative analysis demonstrated a highly significant elevation ($p < 0.001$) in both the frequency of halo-forming cells and the overall percentage of apoptotic cells following $Ca(OH)_2$NPs exposure (Table 3), confirming extensive DNA fragmentation.

These findings were further validated by DAPI staining, which provided detailed insight into nuclear morphology and chromatin organization. Untreated control HCT-116 cancer cells exhibited large, rounded nuclei with uniform fluorescence, reflecting intact chromatin and normal cellular status. In contrast, $Ca(OH)_2$NPs-treated cells displayed characteristic apoptotic features, including marked chromatin condensation, nuclear shrinkage, fragmentation, and the formation of apoptotic bodies, observed as intensely fluorescent, granular structures under fluorescence microscopy (Fig. 6). Consistent with the chromatin diffusion results, quantitative scoring demonstrated a highly significant increase ($p < 0.001$) in the proportion of apoptotic nuclei in $Ca(OH)_2$NPs-treated

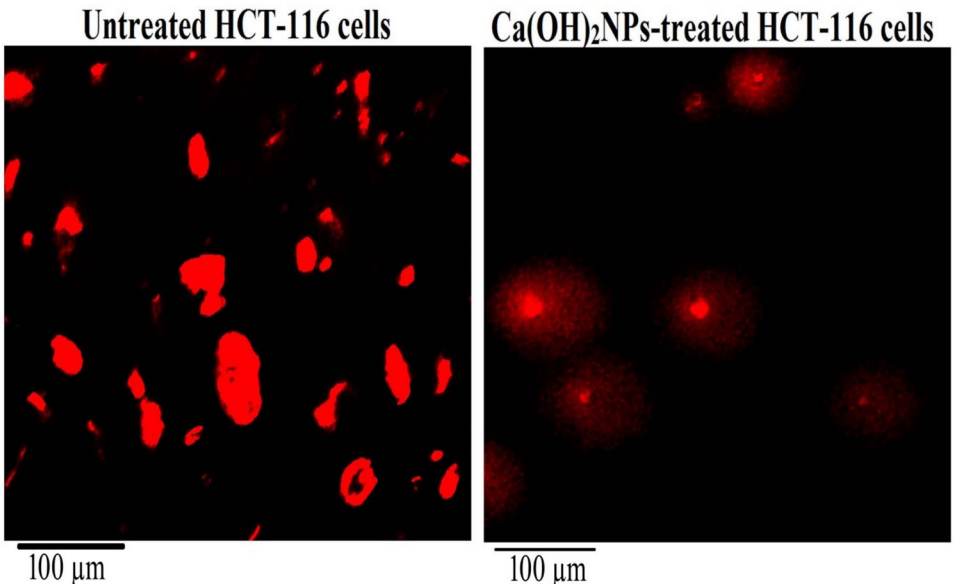

Fig. 5 Chromatin diffusion assay showing intact nuclear DNA in control cells and diffused apoptotic DNA in $Ca(OH)_2$NPs-treated HCT-116 colorectal cancer cells following 72-h exposure to the IC_{50} concentration (35.04 µg/ml). For quantitative analysis, a total of 1000 cells per experimental group were scored across three independent experiments. Magnification: 200×

Table 3 Incidence of apoptosis induction in human HCT-116 colorectal cancer cells detected by chromatin diffusion assay following exposure to the IC_{50} concentration (35.04 µg/ml) of $Ca(OH)_2$NPs for 72 h

Cells	Treatment (concentration)	Number of cells with		Percentage of apoptotic cells
		Intact DNA	Diffused DNA	
HCT-116 colorectal cancer cells	Untreated (0.00 µg/ml)	957.67 ± 10.21	42.33 ± 10.21	4.23 ± 1.03
	$Ca(OH)_2$NPs-treated (35.04 µg/ml)	187.33 ± 7.02***	812.67 ± 7.02***	81.27 ± 0.70***

Triplicates were used and results are expressed as mean ± SD

***Indicates statistical significant difference from the compared untreated control cells at $p < 0.001$, using independent Student t-test

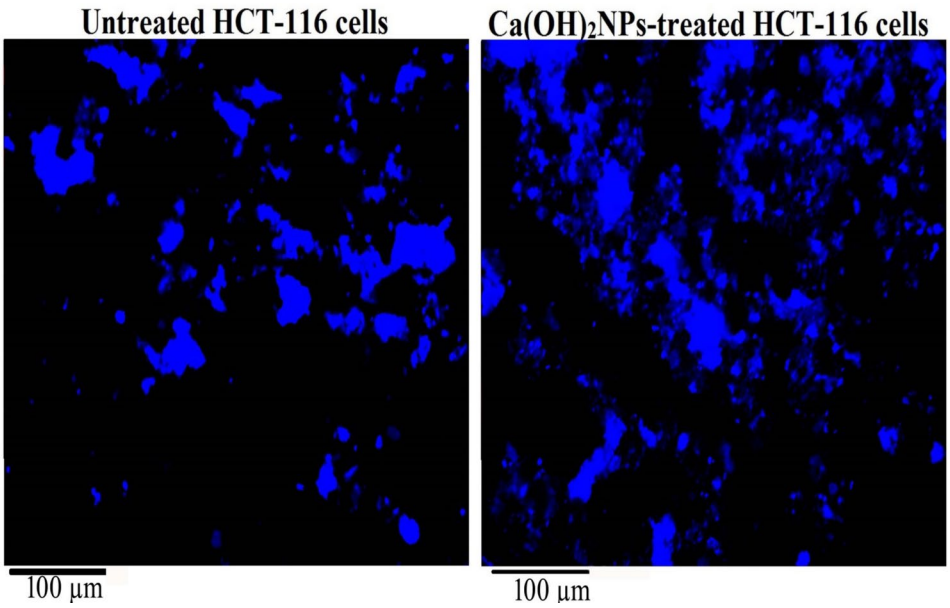

Fig. 6 DAPI staining illustrating intact, uniformly stained nuclei in untreated HCT-116 cells and condensed or fragmented nuclei in $Ca(OH)_2$NPs-treated apoptotic cells following 72-h exposure to the IC_{50} concentration (35.04 µg/ml). A total of 1000 cells per group were evaluated for nuclear morphology assessment across three independent experiments. Magnification: 200×

cells relative to untreated control HCT-116 cancer cells (Table 4). Collectively, the strong consistency between the chromatin diffusion assay and DAPI staining findings provides compelling evidence that $Ca(OH)_2$NPs effectively induce apoptosis in HCT-116 colorectal cancer cells. The evident marked chromatin fragmentation and nuclear disintegration point activation of the intrinsic, mitochondria-mediated apoptotic pathway, likely arising from $Ca(OH)_2$NPs-induced oxidative stress, mitochondrial dysfunction, and genomic instability.

$Ca(OH)_2$NPs significantly dysregulate apoptotic *p53*, mitochondrial *ND3*, and anti-apoptotic *Bcl-2* gene expression in human HCT-116 colorectal cancer cells

Results of qRT-PCR analysis revealed that exposure of HCT-116 colorectal cancer cells to the IC_{50} concentration (35.04 µg/ml) of $Ca(OH)_2$NPs for 72 h induced significant changes in genes regulating apoptosis and mitochondrial function. As shown in Table 5, HCT-116 cell treatment with $Ca(OH)_2$NPs resulted in a highly significant downregulation ($p < 0.001$) of the tumor suppressor and pro-apoptotic gene *p53* compared with untreated control Hct-116 cells, indicating suppression of *p53*-dependent stress and apoptotic pathways. Similarly, the expression of the anti-apoptotic *Bcl-2* gene was significantly downregulated ($p < 0.001$) following exposure to $Ca(OH)_2$NPs at the IC_{50} concentration for 72 h (Table 5). This significant downregulation suggests impairment of mitochondrial protective pathways and indicates a shift in cellular homeostasis toward enhanced pro-apoptotic signaling and mitochondrial dysfunction.

Conversely, the mitochondrial *ND3* gene, an essential subunit of complex I in the mitochondrial electron transport chain, was significantly upregulated ($p < 0.001$) in $Ca(OH)_2$NPs-treated HCT-116 cells relative to untreated control cells (Table 5). This pronounced upregulation likely reflects mitochondrial stress and alterations in respiratory chain activity, potentially representing a compensatory cellular response to impaired oxidative phosphorylation and mitochondrial damage induced by nanoparticle exposure. Collectively, the concurrent significant downregulation of *p53* and *Bcl-2*, together with the pronounced upregulation

Table 4 Apoptosis level in human HCT-116 colorectal cancer cells measured using DAPI staining following exposure to the IC_{50} concentration (35.04 µg/ml) of $Ca(OH)_2$NPs for 72 h

Cells	Treatment (concentration)	Number of cells with		Percentage of apoptotic cells
		Intact DNA	Fragmented and condensed DNA	
HCT-116 colorectal cancer cells	Untreated (0.00 µg/ml)	940.67 ± 9.45	59.33 ± 9.45	5.93 ± 0.94
	$Ca(OH)_2$NPs-treated (35.04 µg/ml)	84.33 ± 10.01***	915.67 ± 10.01***	91.57 ± 1.01***

Triplicates were used and results are expressed as mean ± SD

***Indicates statistical significant difference from the compared untreated control cells at $p < 0.001$, using independent Student t-test

Table 5 The expression level of *p53*, *ND3*, and *Bcl2* genes in human HCT-116 colorectal cancer cells following exposure to the IC_{50} concentration (35.04 µg/ml) of $Ca(OH)_2$NPs for 72 h

Cells	Treatment (concentration)	*p53*	*ND3*	*Bcl2*
HCT-116 colorectal cells	Untreated (0.00 µg/ml)	1.00 ± 0.00	1.00 ± 0.00	1.00 ± 0.00
	$Ca(OH)_2$NPs-treated (35.04 µg/ml)	0.27 ± 0.05***	2.39 ± 0.20***	0.03 ± 0.01***

Results are expressed as mean ± SD

***Indicates statistical significant difference from the compared untreated control cells at $p < 0.001$, using independent Student t-test

of *ND3*, demonstrates a complex molecular response triggered by $Ca(OH)_2$NPs in HCT-116 colorectal cancer cells. These alterations suggest that $Ca(OH)_2$NPs profoundly disturb mitochondrial homeostasis and apoptotic regulatory networks, providing important mechanistic insight into their cytotoxic activity and highlighting their potential as nanotherapeutic agents for colorectal cancer treatment.

Discussion

Nowadays, the potentially valuable biomedical properties of $Ca(OH)_2$NPs, including their highly alkaline nature, strong chemical reactivity, and ability to influence cellular ionic balance and oxidative status, have attracted increasing attention for potential anticancer applications. These distinctive physicochemical characteristics may interfere with critical cellular processes required for cancer cell survival, such as mitochondrial function, genomic stability, and the regulation of apoptotic pathways (Mohamed et al. 2025a, b; Fakeeha et al. 2025). However, despite these promising features, the therapeutic potential and underlying molecular mechanisms of $Ca(OH)_2$NPs in cancer therapy, particularly in colorectal cancer, remain largely unexplored. Colorectal cancer is one of the most prevalent and lethal malignancies worldwide. Conventional chemotherapy, although widely used, is often associated with severe systemic toxicities, including myelosuppression, cardiotoxicity, nephrotoxicity, and neurotoxicity. In addition, traditional chemotherapeutic agents frequently face major challenges such as drug resistance, poor tumor selectivity, and damage to normal proliferating tissues. These limitations substantially compromise treatment efficacy and negatively affect patients' quality of life (Tang et al. 2023; Shin et al. 2023; Zahra et al. 2025). Consequently, the development of novel therapeutic strategies capable of selectively targeting colorectal cancer cells while minimizing systemic adverse effects is urgently needed.

Considering the promising physicochemical properties of $Ca(OH)_2$NPs and the absence of studies investigating their anticancer activity in colorectal cancer, further research is required to clarify their cytotoxic mechanisms and therapeutic potential. Therefore, the present study was conducted to assess the cytotoxic effects of $Ca(OH)_2$NPs in normal HFB4 melanocytes and human HCT-116 colorectal cancer cells. In addition, the study examined their impact on genomic DNA integrity, mitochondrial membrane potential, intracellular ROS generation, and apoptosis induction in HCT-116 colorectal cancer cells. Human colorectal carcinoma HCT-116 cells represent a well-established in vitro model widely used to study colorectal cancer pathophysiology and to evaluate novel therapeutic agents. These cells exhibit several hallmark characteristics of malignancy, including rapid proliferation, evasion of apoptosis, metabolic reprogramming, mitochondrial dysfunction, and elevated oxidative stress levels (Li et al. 2024, 2025). Such features closely mimic the biological behavior of colorectal tumors and therefore make HCT-116 cells a reliable experimental platform for investigating therapies that target oxidative stress, mitochondrial activity, or apoptosis-related signaling pathways.

In the present study, $Ca(OH)_2$NPs exhibited significant cytotoxic activity against HCT-116 colorectal cancer cells while showing negligible toxicity toward normal HFB4 melanocytes (Fig. 7). The MTT cytotoxicity assay demonstrated a pronounced, concentration-dependent reduction in the viability of HCT-116 cells following 72-h exposure to $Ca(OH)_2$NPs across a wide concentration range, whereas only minimal effects on HFB4 cell viability were observed under the same experimental conditions. The 72-h treatment duration was selected based on preliminary optimization experiments and previous nanoparticle cytotoxicity studies indicating that prolonged exposure is often required to achieve sufficient nanoparticle–cell interaction, intracellular accumulation, and measurable downstream cellular responses. In our preliminary observations, shorter exposure periods (24 and 48 h) produced weaker and less consistent cytotoxic effects compared with the more pronounced responses observed after 72 h of exposure (Mohamed et al. 2025a, c). The relatively low IC_{50} value recorded for HCT-116 cells, together with a high selectivity index of 5.44, indicates a strong sensitivity of colorectal cancer cells to $Ca(OH)_2$NPs-induced growth inhibition and highlights the potent antiproliferative activity of these nanoparticles under the present experimental conditions. These findings are consistent with recent reports demonstrating the selective and potent anticancer activity of $Ca(OH)_2$NPs against HepG2 hepatocellular carcinoma cells and PANC-1 pancreatic

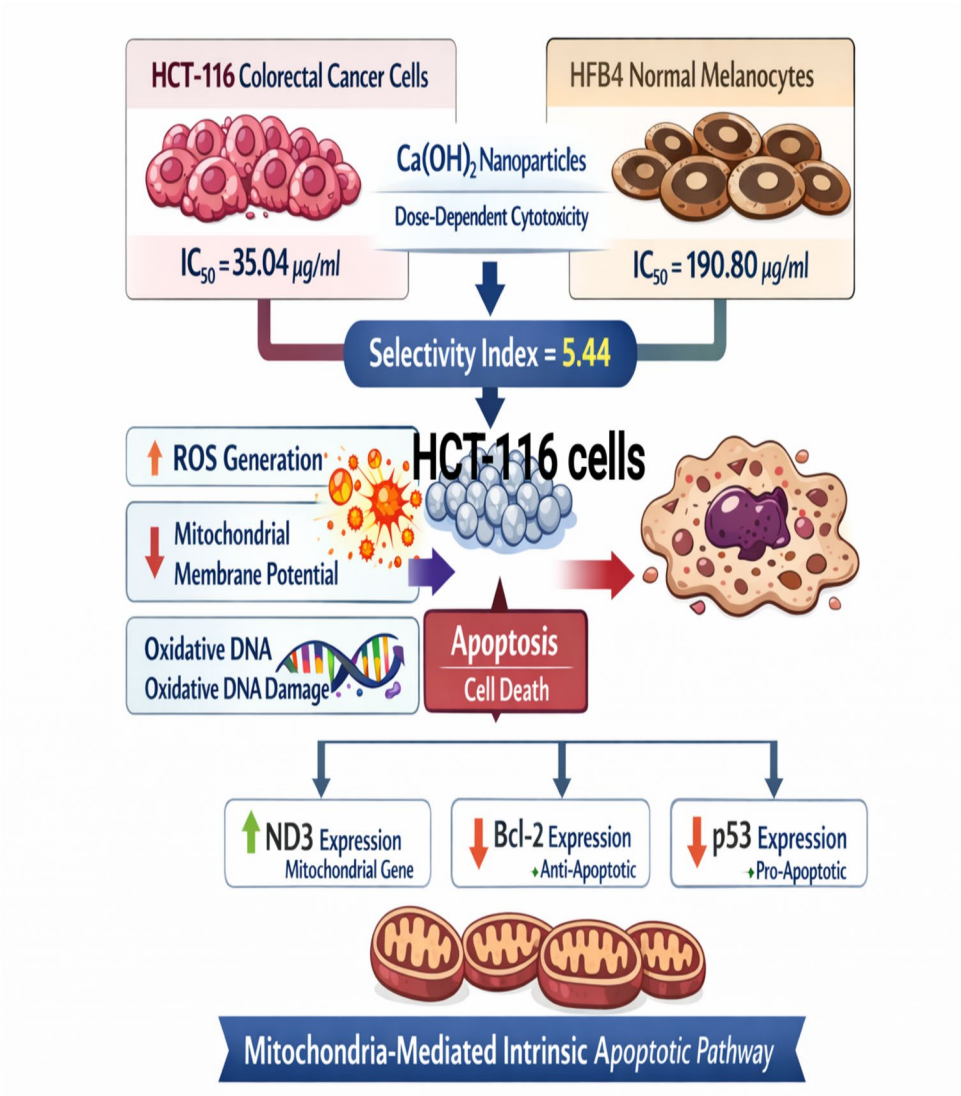

Fig. 7 Mechanistic illustration of $Ca(OH)_2$NPs-induced selective cytotoxicity and mitochondria-mediated apoptosis in HCT-116 colorectal cancer cells

cancer cells, with comparatively minimal toxicity toward normal oral epithelial cells (Mohamed et al. 2025a, b). Nanoparticle-induced cytotoxicity may be more pronounced in malignant cells due to their elevated metabolic activity and increased basal oxidative stress levels, which can enhance their susceptibility to further oxidative imbalance and cellular damage (Mohamed et al. 2025c; Subramaniam et al. 2024). Accordingly, the cytotoxic effects of $Ca(OH)_2$NPs observed in HCT-116 cells may be associated with the increased vulnerability of cancer cells to oxidative and mitochondrial stress compared with normal HFB4 melanocytes.

One of the primary mechanisms underlying nanoparticle-mediated cytotoxicity is the induction of oxidative stress through excessive intracellular generation of ROS. Cancer cells generally maintain higher basal ROS levels than normal cells as a consequence of their hyperactive metabolism and partially impaired mitochondrial function, which makes them particularly susceptible to additional oxidative stress (Subramaniam et al. 2024; Asil and Narayan 2021; Raza et al. 2017; Herdiana et al. 2023). In the present study, fluorometric analysis using the DCFH-DA probe demonstrated a significant increase ($p < 0.001$) in intracellular ROS generation levels in HCT-116 cells following treatment with $Ca(OH)_2$NPs at the IC_{50}concentration. The excessive accumulation of ROS overwhelms the cellular antioxidant defense system, resulting in oxidative damage to essential biomolecules, including lipids, proteins, and nucleic acids. Such oxidative stress acts as a critical upstream trigger that can initiate downstream molecular events, including DNA damage, mitochondrial dysfunction, and the activation of apoptotic signaling pathways (Snezhkina et al. 2019; Liu et al. 2020).

Consistent with the observed oxidative stress, genotoxicity evaluation using the alkaline comet assay demonstrated severe DNA damage in $Ca(OH)_2$NPs-treated HCT-116 cells. The treated cells exhibited pronounced DNA fragmentation,

increased comet tail length, and significantly elevated tail moment values compared with untreated controls, indicating extensive single-strand DNA breaks and genomic instability. Fluorescence microscopic observations further confirmed these findings, as treated cells displayed typical comet structures with elongated DNA tails, whereas control cells retained intact nuclear morphology with minimal DNA migration. The strong association between ROS overproduction and DNA damage observed in this study supports the concept that $Ca(OH)_2$NPs induce lethal oxidative genotoxic stress in colorectal cancer cells.

Genomic instability is a well-recognized consequence of excessive oxidative stress, as elevated ROS levels can directly damage DNA molecules and disrupt the cellular repair mechanisms responsible for preserving genomic integrity (Poetsch 2020; Ayna et al. 2025). Consequently, assessing genomic instability provides critical evidence linking $Ca(OH)_2$NPs-induced oxidative stress with genomic DNA damage in colorectal cancer cells. Assessment of genomic DNA integrity using the alkaline comet assay provides a highly sensitive approach for detecting DNA strand breaks and alkali-labile sites at the single-cell level, making it a reliable indicator of genomic instability (Pu et al. 2015; He et al. 2025). In the present study, the comet assay demonstrated marked genomic DNA damage in HCT-116 cancer cells following treatment with $Ca(OH)_2$NPs, consistent with the increased oxidative stress observed in treated cells. Specifically, $Ca(OH)_2$NPs-exposed cells exhibited pronounced DNA fragmentation, increased comet tail length, and significantly higher tail moment values compared with untreated control cells, indicating extensive single-strand DNA breaks and impaired genomic stability. Fluorescence microscopic examination further supported these findings, revealing distinct comet structures with elongated DNA tails in $Ca(OH)_2$NPs-treated HCT-116 cancer cells, while control cells retained compact nuclei with minimal DNA migration. Collectively, these results consistent with the recent findings of Mohamed et al. (Mohamed et al. 2025a, b) indicate that $Ca(OH)_2$NPs-induced oxidative stress leads to significant DNA strand breaks, thereby promoting genomic instability in colorectal cancer cells.

In addition to damaging nuclear DNA, $Ca(OH)_2$NPs-induced oxidative stress also severely disrupts mitochondrial function. Mitochondria, center of cellular energy production and apoptosis regulation, are highly sensitive to oxidative insults, and the loss of mitochondrial membrane potential represents an early and decisive step in triggering intrinsic apoptotic pathways (Khan et al. 2022; Ye et al. 2025). Rhodamine-123 staining of HCT-116 cancer cells exposed to $Ca(OH)_2$NPs for 72 h revealed marked depolarization of mitochondrial membranes, reflecting significant disruption of mitochondrial bioenergetics, including collapse of the proton gradient required for ATP synthesis. This mitochondrial dysfunction is likely driven by excessive ROS generated in response to $Ca(OH)_2$NPs, which damages mitochondrial membranes, impairs electron transport chain function, and triggers the opening of mitochondrial permeability transition pores. Altogether, these alterations lead to severe mitochondrial impairment and enhance apoptotic signaling in $Ca(OH)_2$NPs-treated colorectal HCT-116 cells (Mohamed et al. 2025b; Guo et al. 2013; Ho and Shirakawa 2022).

The genomic instability and mitochondrial dysfunction induced by excessive ROS generation observed in this study forced HCT-116 colorectal cancer cells toward apoptotic cell death. The induction of apoptosis in $Ca(OH)_2$NPs-treated HCT-116 cancer cells was confirmed using two complementary techniques: the chromatin diffusion assay and DAPI nuclear staining. Both assays demonstrated typical apoptotic nuclear alterations in $Ca(OH)_2$NPs-treated cells, including chromatin condensation, nuclear shrinkage, formation of apoptotic bodies, and nuclear fragmentation. These findings are consistent with previous studies reporting similar apoptotic morphological features after exposure of triple-negative breast cancer MDA-MB-231 cells and Hep-G2 hepatocellular carcinoma cells to bioactive glass nanoparticles (5Mohamed et al. 2025d). The chromatin diffusion assay enabled sensitive detection of apoptotic DNA dispersion, whereas DAPI staining allowed clear visualization of nuclear morphological changes associated with apoptosis. Moreover, the absence of necrotic morphological features indicates that the cytotoxic activity of $Ca(OH)_2$NPs predominantly occurs through regulated apoptotic mechanisms rather than nonspecific cellular damage (Mandelkow et al. 2017).

Results of qRT-PCR analysis provided further mechanistic insight into the molecular response of HCT-116 cancer cells to $Ca(OH)_2$NPs exposure. Treatment with $Ca(OH)_2$NPs resulted in significant dysregulation in the expression of critical genes involved in apoptosis regulation and mitochondrial function. Notably, the tumor suppressor *p53* and the anti-apoptotic *Bcl-2* genes were significantly downregulated, whereas the mitochondrial *ND3* gene was markedly upregulated. The *ND3* encodes a core subunit of NADH dehydrogenase (complex I) within the mitochondrial electron transport chain and plays a crucial role in mitochondrial respiration. Alterations in *ND3*expression are often associated with mitochondrial respiratory stress and disruption of electron transport chain activity (Jin et al. 2018; Bennett et al. 2022). Overexpression of*ND3* can disrupt the normal assembly and function of mitochondrial complex I, leading to inefficient electron transfer within the respiratory chain. This dysfunction promotes electron leakage from complex I to molecular oxygen, resulting in excessive mitochondrial ROS generation. The elevated ROS levels intensify oxidative stress, damage mitochondrial structures, and compromise

the mitochondrial membrane potential. Consequently, these mitochondrial perturbations trigger intrinsic apoptotic signaling pathways, ultimately promoting apoptosis in cancer cells (Okoye et al. 2023; Zong et al. 2024).

Moreover, the simultaneous significant downregulation of *Bcl-2*, which normally preserves mitochondrial membrane integrity, and *p53*, which regulates cellular stress responses, further sensitizes cells to mitochondrial dysfunction and apoptosis. Together, these transcriptional alterations highlight profound disruption of mitochondrial homeostasis and apoptotic regulatory networks in $Ca(OH)_2$NPs-treated HCT-116 cells. The observed significant reduction in *Bcl-2* expression, a critical protein responsible for preserving mitochondrial membrane integrity and inhibiting apoptosis, indicates suppression of cellular survival pathways and increased vulnerability to mitochondrial-mediated apoptotic signaling. Although *p53* is widely recognized as a pro-apoptotic tumor suppressor, its downregulation under severe oxidative stress conditions may reflect disruption of normal p53-dependent stress-response pathways. In such circumstances, apoptosis can still proceed through mitochondrial dysfunction associated with excessive ROS generation, and the loss of anti-apoptotic protection resulting from Bcl-2 suppression. Collectively, these transcriptional alterations reflect substantial disturbance of mitochondrial homeostasis and apoptotic regulatory networks in $Ca(OH)_2$NPs-treated HCT-116 cells, ultimately favoring the activation of mitochondrial-driven apoptotic pathways.

Furthermore, the pronounced downregulation of *Bcl-2* and *p53* observed in $Ca(OH)_2$NPs-treated HCT-116 cancer cells further increases cellular susceptibility to mitochondrial dysfunction and apoptotic cell death. *Bcl-2*is a pivotal anti-apoptotic gene that maintains mitochondrial membrane integrity, prevents cytochrome c release, and inhibits the initiation of intrinsic apoptotic pathway (Qian et al. 2022; Vogler et al. 2025). Therefore, the significant reduction in*Bcl-2* expression detected in $Ca(OH)_2$NPs-treated HCT-116 cells in this study indicates disruption of critical cellular survival mechanisms. This loss of anti-apoptotic protection renders mitochondria more susceptible to oxidative damage and promotes the activation of mitochondria-dependent apoptotic signaling. Simultaneously, a significant downregulation of *p53* was observed in $Ca(OH)_2$NPs-treated HCT-116 cancer cells. As a critical tumor suppressor involved in DNA damage sensing, cell cycle regulation, and apoptosis induction, the significant reduction of *p53* expression may indicate an altered cellular stress-response state under conditions of pronounced oxidative and mitochondrial stress induced by $Ca(OH)_2$NPs exposure (Hernández Borrero and El-Deiry 2021; Zhang et al. 2024). Nevertheless, apoptotic cell death may still proceed independently of*p53*, particularly in the presence of mitochondrial dysfunction, excessive ROS generation, and suppression of the anti-apoptotic *Bcl-2* gene. Collectively, these gene expression alterations suggest disruption of mitochondrial and apoptotic regulatory balance rather than activation of a defined signaling cascade. Overall, the combined effects of oxidative stress, mitochondrial impairment, and altered apoptosis-related gene expression are consistent with the induction of mitochondria-associated apoptotic cell death in HCT-116 cancer cells.

The findings discussed above therefore demonstrate that $Ca(OH)_2$NPs exhibit strong and targeted anticancer activity against colorectal cancer cells through a multifaceted mechanism involving excessive ROS generation, oxidative DNA damage, mitochondrial dysfunction, and activation of apoptotic pathways (Fig. 7). The integrated relationship between oxidative stress, genomic instability, and mitochondrial impairment provides a coherent mechanistic explanation for the cytotoxic effects of $Ca(OH)_2$NPs in HCT-116 colorectal cancer cells. A major strength of this study lies in the comprehensive evaluation of the anticancer potential of $Ca(OH)_2$NPs toward HCT-116 cells through the integration of multiple experimental approaches, including cytotoxicity, oxidative stress, genotoxicity, mitochondrial function, apoptosis assessment, and molecular gene expression analyses. This integrative strategy enabled the establishment of a detailed mechanistic framework describing the $Ca(OH)_2$NPs-mediated anticancer activity.

Despite these significant findings, certain limitations should be considered. The current study was performed using a single colorectal cancer cell line under in vitro conditions, which may not fully reflect the biological complexity and heterogeneity of colorectal tumors in vivo. In addition, the comparison with HFB4 melanocytes does not provide a tissue-matched normal intestinal model for fully assessing selective anticancer activity. Furthermore, although Ca(OH)2NPs induced marked cytotoxicity and oxidative cellular damage, the potential contribution of nanoparticle-associated alkalinity was not specifically evaluated through direct pH monitoring or buffering controls. The molecular analyses performed in this study were also limited to the assessment of selected apoptosis- and mitochondria-related genes without pathway-specific validation experiments; therefore, the precise molecular mechanisms underlying the observed effects remain to be fully elucidated. Accordingly, further investigations using additional colorectal cancer models, normal intestinal epithelial cell lines, mechanistic pathway analyses, and in vivo experimental systems are necessary to validate the selectivity, therapeutic efficacy, biodistribution, pharmacokinetics, biocompatibility, and long-term safety profile of $Ca(OH)_2$NPs before considering potential clinical applications. Nevertheless, the results of this study provide strong evidence that Ca(OH)2NPs represent a potential nanotherapeutic candidate for colorectal

cancer treatment, supporting the need for further preclinical investigations to advance their development toward potential clinical applications.

Conclusion

This study demonstrates, for the first time, that $Ca(OH)_2$NPs exert potent anticancer activity against HCT-116 colorectal cancer cells, while exhibiting minimal toxicity toward normal HFB4 melanocytes. This cytotoxicity is mediated by excessive ROS generation, which induces oxidative DNA damage, disrupts mitochondrial function, and alters the expression of apoptosis- and mitochondria-related genes, ultimately activating intrinsic apoptotic pathways in HCT-116 cells. A novel aspect of this work lies in the comprehensive mechanistic analysis, integrating cytotoxicity, oxidative stress, genotoxicity, mitochondrial integrity, apoptosis evaluation, and molecular gene expression, which collectively provide a detailed framework for understanding how $Ca(OH)_2$NPs mediate anticancer effects. Despite these important findings, some limitations should be acknowledged. The study was performed using a single colorectal cancer cell line under in vitro conditions, which may not fully replicate the complexity, heterogeneity, or tumor microenvironment of colorectal cancer in vivo. Furthermore, the long-term effects, cellular uptake dynamics, and potential off-target toxicity of $Ca(OH)_2$NPs were not addressed and require further investigation. Future studies should focus on validating these findings in additional colorectal cancer models and in vivo systems, assessing the pharmacokinetics, biodistribution, and safety profile of $Ca(OH)_2$NPs, and exploring their long-term cytotoxic effects and molecular interactions. Investigating targeted delivery strategies and combination therapies may further enhance the translational potential of $Ca(OH)_2$NPs as a potent nanotherapeutic approach for colorectal cancer. In summary, this study provides compelling evidence that $Ca(OH)_2$NPs are a potent candidate for colorectal cancer therapy, offering a novel mechanistic insight into their potential anticancer activity and laying the groundwork for future preclinical development.

Acknowledgements We sincerely thank the Department of Zoology, Faculty of Science, Cairo University, for their generous provision of the essential chemicals and equipment used in this study. Their valuable support and collaboration were instrumental in facilitating the successful execution of our experiments, and we are deeply grateful for their contribution to our research.

Author contribution Hanan R.H. Mohamed conceived and designed the study, conducted molecular experiments, performed statistical analyses, and drafted the manuscript. Rawan S. Hekal, Chahd W.H. Fahmy, Shahd O. Elhaggan, Zeina Noure, and Nada Ahmed carried out experimental work and contributed to manuscript writing. Ayman Diab, Gehan Safwat and all other authors reviewed and approved the final version of the manuscript. The authors declare that all data were generated in-house and that no paper mill was used.

Funding The current study was partially funded by the Faculty of Science, Cairo University, and the Faculty of Biotechnology at October University for Modern Sciences and Arts (MSA), Egypt.

Data availability The datasets used and/or analyzed during the current study are available from the corresponding author on reasonable request.

Code availability Not applicable.

Declarations

Consent to participate Not applicable.

Consent for publication Not applicable.

Competing interests The authors declare no competing interests.

References

Abdelsalam EA, Abd El-Hafeez AA, Eldehna WM, El Hassab MA, Marzouk HMM, Elaasser MM, Abou Taleb NA, Amin KM, Abdel-Aziz HA, Ghosh P, Hammad SF (2022) Discovery of novel thiazolyl-pyrazolines as dual EGFR and VEGFR-2 inhibitors endowed with in vitro antitumor activity towards non-small lung cancer. J Enzyme Inhib Med Chem 37(1):2265–2282. https://doi.org/10.1080/14756366.2022.2104841

Ammar MM, Ali R, Abd Elaziz NA, Habib H, Abbas FM, Yassin MT, Maniah K, Abdelaziz R (2025) Nanotechnology in oncology: advances in biosynthesis, drug delivery, and theranostics. Discov Oncol 16(1):1172.https://doi.org/10.1007/s12672-025-02664-3

Anand U, Dey A, Chandel AKS, Sanyal R, Mishra A, Pandey DK, De Falco V, Upadhyay A, Kandimalla R, Chaudhary A, Dhanjal JK, Dewanjee S, Vallamkondu J, Pérez de la Lastra JM (2022) Cancer chemotherapy and beyond: current status, drug candidates, associated risks and progress in targeted therapeutics. Genes Dis 10(4):1367–1401.https://doi.org/10.1016/j.gendis.2022.02.007

Anbari K, Ghanadi K (2025) Colorectal cancer: risk factors, novel approaches in molecular screening and treatment. Int J Mol Cell Med 14(1):576–605.https://doi.org/10.22088/IJMCM.BUMS.14.1.576

Asil SM, Narayan M (2021) The multifaceted function of nanoparticles in modulating oxidative stress in cancer therapy. In: Chakraborti S (ed) Handbook of oxidative stress in cancer: therapeutic aspects. Springer, Singapore. https://doi.org/10.1007/978-981-16-1247-3_115-1

Ayna A, Caglayan C, Taysi S (2025) Cellular and molecular mechanisms of oxidative DNA damage and repair. Medicina (Kaunas) 61(11):2013. https://doi.org/10.3390/medicina61112013

Bennett CF, Latorre-Muro P, Puigserver P (2022) Mechanisms of mitochondrial respiratory adaptation. Nat Rev Mol Cell Biol 23(12):817–835.https://doi.org/10.1038/s41580-022-00506-6

Bishoyi AK, Nouri S, Hussen A, Bayani A, Khaksari MN, Soleimani Samarkhazan H (2025) Nanotechnology in leukemia therapy: revolutionizing targeted drug delivery and immune modulation. Clin Exp Med 25(1):166.https://doi.org/10.1007/s10238-025-01686-z

El-Zahabi HSA, Khalifa MMA, Gado YMH, Farrag AM, Elaasser MM, Safwat NA, AbdelRaouf RR, Arafa RK (2019) New thiobarbituric acid scaffold-based small molecules: synthesis, cytotoxicity,

2D-QSAR, pharmacophore modelling and in-silico ADME screening. Eur J Pharm Sci 130:124–136.https://doi.org/10.1016/j.ejps.2019.01.023

Fadlallah H, El Masri J, Fakhereddine H, Youssef J, Chemaly C, Doughan S, Abou-Kheir W (2024) Colorectal cancer: recent advances in management and treatment. World J Clin Oncol 15(9):1136–1156.https://doi.org/10.5306/wjco.v15.i9.1136

Fakeeha G, Al-Zamil L, Muthurangan M, Auda S, Balto H (2025) Size-dependent bioactivity of silver nanoparticles and calcium hydroxide mixtures against hDPSCs: An in vitro study. Int J Mol Sci 26(21):10604. https://doi.org/10.3390/ijms262110604

Gharib E, Robichaud GA (2024) From crypts to cancer: a holistic perspective on colorectal carcinogenesis and therapeutic strategies. Int J Mol Sci 25(17):9463.https://doi.org/10.3390/ijms25179463

Grzybowska-Szatkowska L, Ślaska B (2014) Mitochondrial NADH dehydrogenase polymorphisms are associated with breast cancer in Poland. J Appl Genet 55:173–181

Guan X, Guan Y (2020) Artemisinin induces selective and potent anticancer effects in drug resistant breast cancer cells by inducing cellular apoptosis and autophagy and G2/M cell cycle arrest. J BUON 25(3):1330–1336

Guo C, Sun L, Chen X, Zhang D (2013) Oxidative stress, mitochondrial damage and neurodegenerative diseases. Neural Regen Res 8(21):2003–2014.https://doi.org/10.3969/j.issn.1673-5374.2013.21.009

He X, Chen F, Zhou L, Sun Y, Liu Q, Chen W, Zhu L, Zhang J, Zhu WG (2025) The comet assay: a contemporary approach for detecting genomic instability. DNA Repair (Amst) 154:103899. https://doi.org/10.1016/j.dnarep.2025.103899

Herdiana Y, Sriwidodo S, Sofian FF, Wilar G, Diantini A (2023) Nanoparticle-based antioxidants in stress signaling and programmed cell death in breast cancer treatment. Molecules 28(14):5305. https://doi.org/10.3390/molecules28145305

Hernández Borrero LJ, El-Deiry WS (2021) Tumor suppressor p53: biology, signaling pathways, and therapeutic targeting. Biochim Biophys Acta Rev Cancer 1876(1):188556.https://doi.org/10.1016/j.bbcan.2021.188556

Ho HJ, Shirakawa H (2022) Oxidative stress and mitochondrial dysfunction in chronic kidney disease. Cells 12(1):88.https://doi.org/10.3390/cells12010088

Jin EH, Sung JK, Lee SI, Hong JH (2018) Mitochondrial NADH dehydrogenase subunit 3 (MTND3) polymorphisms are associated with gastric cancer susceptibility. Int J Med Sci 15(12):1329–1333.https://doi.org/10.7150/ijms.26881

Jung G, Hernández-Illán E, Moreira L, Balaguer F, Goel A (2020) Epigenetics of colorectal cancer: biomarker and therapeutic potential. Nat Rev Gastroenterol Hepatol 17(2):111–130.https://doi.org/10.1038/s41575-019-0230-y

Khan T, Waseem R, Zehra Z, Aiman A, Bhardwaj P, Ansari J, Hassan MI, Islam A (2022) Mitochondrial dysfunction: pathophysiology and mitochondria-targeted drug delivery approaches. Pharmaceutics 14(12):2657. https://doi.org/10.3390/pharmaceutics14122657

Langie SA, Azqueta A, Collins AR (2015) The comet assay: past, present, and future. Front Genet 6:266

Lai CY, Tsai AC, Chen MC, Chang LH, Sun HL, Chang YL, Chen CC, Teng CM, Pan SL (2013) Aciculatin induces p53-dependent apoptosis via mdm2 depletion in human cancer cells in vitro and in vivo. PLoS ONE 7(8):e42192

Lao VV, Grady WM (2011) Epigenetics and colorectal cancer. Nat Rev Gastroenterol Hepatol 8(12):686–700.https://doi.org/10.1038/nrgastro.2011.173

Li J, Pan J, Wang L, Ji G, Dang Y (2025) Colorectal cancer: Pathogenesis and targeted therapy. MedComm (2020) 6(3):e70127. https://doi.org/10.1002/mco2.70127

Li Q, Geng S, Luo H, Wang W, Mo YQ, Luo Q, Wang L, Song GB, Sheng JP, Xu B (2024) Signaling pathways involved in colorectal cancer: Pathogenesis and targeted therapy. Signal Transduct Target Ther 9(1):266. https://doi.org/10.1038/s41392-024-01953-7

Liu S, Liu J, Wang Y, Deng F, Deng Z (2020) Oxidative stress: signaling pathways, biological functions, and disease. MedComm (2020) 6(7):e70268. https://doi.org/10.1002/mco2.70268

Mandelkow R, Gümbel D, Ahrend H, Kaul A, Zimmermann U, Burchardt M, Stope MB (2017) Detection and quantification of nuclear morphology changes in apoptotic cells by fluorescence microscopy and subsequent analysis of visualized fluorescent signals. Anticancer Res 37(5):2239–2244.https://doi.org/10.21873/anticanres.11560

Mohamed HRH, Borai ME, Mosaad S, Osman AA, Elsewedy AH, Zaki HM, Diab A, Safwat G (2026) Bioactive glass nanoparticles induce intrinsic p53-dependent apoptosis and promote genomic instability via ROS overproduction and mitochondrial depolarization in triple-negative breast cancer cells. Sci Rep 16(1):809.https://doi.org/10.1038/s41598-025-32827-9

Mohamed HRH, Ibrahim EH, Shaheen SEE, Hussein NOE, Diab A, Safwat G (2025a) Calcium hydroxide nanoparticles induce cell death, genomic instability, oxidative stress and apoptotic gene dysregulation on human HepG2 cells. Sci Rep 15(1):2993.https://doi.org/10.1038/s41598-025-86401-4

Mohamed HRH, Magdy H, Elberry Y, Ismail M, Michael M, Eltayeb N, Safwat G, Diab A (2025b) Calcium hydroxide nanoparticles induce apoptotic cell death in human pancreatic cancer cells through over ROS-driven genomic instability and mitochondrial dysfunction. Sci Rep 15(1):40356.https://doi.org/10.1038/s41598-025-26135-5

Mohamed HRH, Osman AA, Mosaad S, Elsewedy AH, Zaki HM, Borai ME, Aref AM, Safwat G (2025d) Bioactive glass nanoparticles induce pronounced cytotoxicity in human hepatocellular carcinoma Hep-G2 cells through ROS-mediated genomic instability and mitochondrial apoptosis. Naunyn Schmiedebergs Arch Pharmacol. https://doi.org/10.1007/s00210-025-04731-6

Mohamed HRH, Shaheen SEE, Ibrahim EH, Hussein NOE, Safwat G (2025c) Calcium titanate nanoparticles-induced cytotoxicity, genotoxicity and oxidative stress in human non-small lung cancer cells. Sci Rep 15(1):6373. https://doi.org/10.1038/s41598-025-89035-8

Mosmann T (1983) Rapid colorimetric assay for cellular growth and survival: application to proliferation and cytotoxicity assays. J Immunol Methods 65:55–63

Okoye CN, Koren SA, Wojtovich AP (2023) Mitochondrial complex I ROS production and redox signaling in hypoxia. Redox Biol 67:102926.https://doi.org/10.1016/j.redox.2023.102926

Poetsch AR (2020) The genomics of oxidative DNA damage, repair, and resulting mutagenesis. Comput Struct Biotechnol J 18:207–219. https://doi.org/10.1016/j.csbj.2019.12.013

Pu X, Wang Z, Klaunig JE (2015) Alkaline comet assay for assessing DNA damage in individual cells. Curr Protoc Toxicol 65:3.12.1-3.12.11. https://doi.org/10.1002/0471140856.tx0312s65

Qian S, Wei Z, Yang W, Huang J, Yang Y, Wang J (2022) The role of BCL-2 family proteins in regulating apoptosis and cancer therapy. Front Oncol 12:985363.https://doi.org/10.3389/fonc.2022.985363

Rattanakijkamol P, Promta P, Wanachantararak P, Leelapornpisid W (2025) Effectiveness of novel calcium hydroxide nanoparticles in the different vehicles against mixed-species biofilm: an in vitro and ex vivo study. J Contemp Dent Pract 26(3):265–272.https://doi.org/10.5005/jp-journals-10024-3846

Rawla P, Sunkara T, Barsouk A (2019) Epidemiology of colorectal cancer: incidence, mortality, survival, and risk factors. Gastroenterol Rev 14(2):89–103.https://doi.org/10.5114/pg.2018.81072

Raza MH, Siraj S, Arshad A, Waheed U, Aldakheel F, Alduraywish S, Arshad M (2017) ROS-modulated therapeutic approaches in cancer treatment. J Cancer Res Clin Oncol 143(9):1789–1809. https://doi.org/10.1007/s00432-017-2464-9

Roig X, Halbaut L, Elmsmari F, Pareja R, Arrien A, Duran-Sindreu F, Delgado LM, Espina M, García ML, Sánchez JAG, Sánchez-López E (2024) Calcium hydroxide-loaded nanoparticles dispersed in thermosensitive gel as a novel intracanal medicament. Int Endod J 57(7):907–921.https://doi.org/10.1111/iej.14041

Shin AE, Giancotti FG, Rustgi AK (2023) Metastatic colorectal cancer: Mechanisms and emerging therapeutics. Trends Pharmacol Sci 44(4):222–236. https://doi.org/10.1016/j.tips.2023.01.003

Siddiqui MA, Kashyap MP, Kumar V, Al-Khedhairy AA, Musarrat J, Pant AB (2010) Protective potential of trans-resveratrol against 4-hydroxynonenal induced damage in PC12 cells. Toxicol in Vitro 24(6):1592–1598.https://doi.org/10.1016/j.tiv.2010.06.008

Singh NP (2000) A simple method for accurate estimation of apoptotic cells. Exp Cell Res 256(1):328–337.https://doi.org/10.1006/excr.2000.4810

Snezhkina AV, Kudryavtseva AV, Kardymon OL, Savvateeva MV, Melnikova NV, Krasnov GS, Dmitriev AA (2019) ROS generation and antioxidant defense systems in normal and malignant cells. Oxid Med Cell Longev 2019:6175804. https://doi.org/10.1155/2019/6175804

Subramaniam H, Lim CK, Tey LH, Wong LS, Djearamane S (2024) Oxidative stress-induced cytotoxicity of HCC2998 colon carcinoma cells by ZnO nanoparticles synthesized from *Calophyllum teysmannii*. Sci Rep 14(1):30198. https://doi.org/10.1038/s41598-024-81384-0

Suzuki K, Kazui T, Yoshida M, Uno T, Kobayashi T, Kimura T, Yoshida T, Sugimura H (1999) Drug-induced apoptosis and p53, BCL-2 and BAX expression in breast cancer tissues in vivo and in fibroblast cells in vitro. Jpn J Clin Oncol 29(7):323–331. https://doi.org/10.1093/jjco/29.7.323

Tang YL, Li DD, Duan JY, Sheng LM, Wang X (2023) Resistance to targeted therapy in metastatic colorectal cancer: Current status and new developments. World J Gastroenterol 29(6):926–948. https://doi.org/10.3748/wjg.v29.i6.926

Tice RR, Agurell E, Anerson D, Burlinson B, Hartmann A, Kobayashi H et al (2000) Single cell gel/comet assay: guidelines for in vitro and in vivo genetic toxicology testing. Environ Mol Mutagen 35:206–221

Vogler M, Braun Y, Smith VM, Westhoff MA, Pereira RS, Pieper NM, Anders M, Callens M, Vervliet T, Abbas M, Macip S, Schmid R, Bultynck G, Dyer MJ (2025) The BCL2 family: from apoptosis mechanisms to new advances in targeted therapy. Signal Transduct Target Ther 10(1):91. https://doi.org/10.1038/s41392-025-02176-0

Xi Y, Xu P (2021) Global colorectal cancer burden in 2020 and projections to 2040. Transl Oncol 14(10):101174.https://doi.org/10.1016/j.tranon.2021.101174

Ye L, Fu X, Li Q (2025) Mitochondrial quality control in health and disease. MedComm (2020) 6(8):e70319. https://doi.org/10.1002/mco2.70319

Zafar A, Khatoon S, Khan MJ, Abu J, Naeem A (2025) Advancements and limitations in traditional anti-cancer therapies: a comprehensive review of surgery, chemotherapy, radiation therapy, and hormonal therapy. Discov Oncol 16(1):607.https://doi.org/10.1007/s12672-025-02198-8

Zahra M, Zahra UB, Abrahamse H, George BP (2025) Overcoming colorectal cancer and cancer stem cell resistance with photodynamic therapy: New frontiers in oncology. RSC Adv 15(45):37833–37855. https://doi.org/10.1039/d5ra07380d

Zhang H, Xu J, Long Y, Maimaitijiang A, Su Z, Li W, Li J (2024) Unraveling the guardian: p53's multifaceted role in the DNA damage response and tumor treatment strategies. Int J Mol Sci 25(23):12928. https://doi.org/10.3390/ijms252312928

Zhang Y, Jiang L, Jiang L, Geng C, Li L, Shao J, Zhong L (2011) Possible involvement of oxidative stress in potassium bromate-induced genotoxicity in human HepG2 cells. Chem Biol Interact 189(3):186–191

Zong Y, Li H, Liao P, Chen L, Pan Y, Zheng Y, Zhang C, Liu D, Zheng M, Gao J (2024) Mitochondrial dysfunction: mechanisms and advances in therapy. Signal Transduct Target Ther 9(1):124.https://doi.org/10.1038/s41392-024-01839-8

Authors and Affiliations

Hanan R. H. Mohamed[1] · Rawan S. Hekal[2] · Chahd W. H. Fahmy[2] · Shahd O. Elhaggan[2] · Zeina Noure[2] · Nada Ahmed[2] · Ayman Diab[2] · Gehan Safwat[2]

✉ Hanan R. H. Mohamed
hananeeyra@cu.edu.eg

[1] Department of Zoology, Faculty of Science, Cairo University, Giza, Egypt

[2] Faculty of Biotechnology, October University for Modern Sciences and Arts (MSA), 6th of October City, Egypt